ACS APPLIED MATERIALS & INTERFACES

Research Article

www.acsami.org

Switching the Biointerface of Displaceable Poly-*p*-xylylene Coatings

Zhen-Yu Guan,† Chih-Yu Wu,† Yi-Jye Li, and Hsien-Yeh Chen*

Department of Chemical Engineering, National Taiwan University, Taipei 10617, Taiwan

Supporting Information

ABSTRACT: A new class of functionalized poly-*p*-xylyene coating has been synthesized to provide switchable and displaceable surface properties for biomaterials. The switchability is achieved through a mechanism for detaching/attaching biomolecules and/or a mechanism through which the programmed restoration of functions or their replacement by other functions can be carried out. This advanced version of poly-*p*-xylylene comprises an integrated disulfide moiety within the functional side group, and the switching phenomenon between the immobilized functional molecules is triggered by the redox thiol−disulfide interchange reaction. These dynamically well-defined molecules on the surfaces respond simultaneously to altered biological properties and controlled biointerfacial functions, for example, switching wettability or reversibly altered cell adhesion activity. Poly-*p*-xylylenes are a key player in controlling surface properties for many important applications, such as medical implants, biosensors, bioMEMS devices, and microfluidics. The introduction of this new facet of poly-*p*-xylylenes enables the dynamic mimicry of biological functions relevant to the design of new biomaterials.

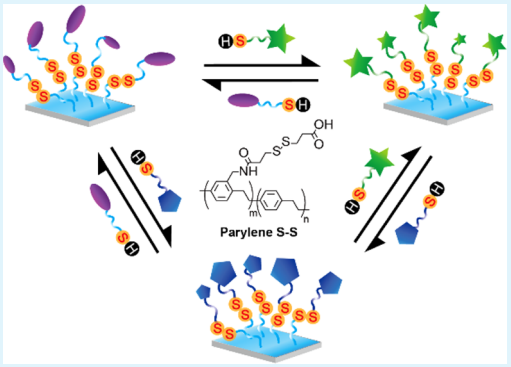

KEYWORDS: *switchable surface, dynamic biointerface, functionalized poly p-xylylene, biomaterials, surface modification*

INTRODUCTION

When biomaterials were initially discovered, the influence of material properties on cell fate decisions and tissue development or regeneration could only be hypothesized.[1,2] Current research has shown that this influence heavily depends not only on the micro- and nanoenvironments of the material surface[3,4] but also on the dynamic effects of surface properties, such as wettability, stiffness, topography, and the immobilized biomolecules, on cells.[5] These effects can be achieved and used to stimulate and control biological functions both *in vitro* and *in vivo*.[6] The emerging concept of mimicking biological systems via molecular remodeling or conformational shifts in a material surface in response to environmental triggers, such as host−guest interactions[7] or stimuli-responsive mechanism,[8] is being used in advanced biointerface design. However, understanding the mechanisms of cell responses to such dynamic and evolving environments still requires further study and investigation.

Poly-*p*-xylylene is a widely used interface material that has been part of the biomaterials revolution. As an FDA-approved material (FDA = U.S. Food and Drug Administration), poly-*p*-xylylene has important applications in medical implants, biosensors, bioMEMS devices, and microfluidics. Several evolved versions of poly-*p*-xylylenes have been produced with enhanced hydrophobicity (Parylene-HT),[9] enhanced optical properties of Parylene-E,[10] and a substrate-dependent deposition of these coatings.[11,12] Additional research has been reported describing the induction of chemical functions on poly-*p*-xylylene surfaces. A more advanced version that has shown promise with regard to biomimicry was devised by a direct synthesis of a target-specific functional and/or combined multifunction on the poly-*p*-xylylene during the vapor-based polymerization process.[13−19] More importantly, the coating technology and proven immobilization method can easily be transferred from one substrate to another.[20−23] However, although the aforementioned dynamic functions have been achieved for the design of novel biointerface materials, the current poly-*p*-xylylene chemistry lacks dynamic control features such as the flexibility to respond to external stimuli, self-restoration of biofunctions, and a dynamic and sustained displacement with new functions.

In this report, we describe an advanced version of poly-*p*-xylylene that features switchable biointerface functions and enables dynamic control over surface chemical properties. Important biointerface criteria including switching wettability and reversibly imparted cell adhesion properties are also demonstrated. This new version of poly-*p*-xylylene contains functional anchoring sites comparable to those of its predecessors. However, it additionally integrates with a disulfide tethered within the functional moieties. The integrated disulfides can be cleaved via a redox stimulus and/or undergo thiol−disulfide interchange reactions via hydrogen exchange and intramolecular cyclization in the presence of other active thiols.[24,25] The redox and thiol-responsive disulfide can be activated specifically under mild conditions using reagents such as dithiothreitol (DTT) or by millimolar-concentrated glutathione (GSH) within the intracellular environment,[26−28]

Received: April 16, 2015
Accepted: June 17, 2015
Published: June 17, 2015

DOI: 10.1021/acsami.5b03286
ACS Appl. Mater. Interfaces 2015, 7, 14431−14438

both of which have been proven to be effective for many drug-eluting systems.[29] This new facet of poly-*p*-xylylene provides it with the ability to participate in the dynamic control of biointerfacial properties. In other words, the biointerfacial properties of the modified surfaces can be programmed via thiol-redox or interchange reactions and are displaceable between thiol-terminated biofunctional molecules or cysteine-functionalized peptide sequences. More importantly, the switchable properties well-mimic biological responses in real time from an interacting cell-adherent state to a noninteractive cell-repellent state, or vice versa, and the switching between these dynamic properties is reversible for a number of cycles. This advanced coating technology provides a dynamically programmable design criterion for biomaterials. Additionally, through the design of thiol-terminated functional molecules, other properties with specific functions of interests can be included.

EXPERIMENTAL SECTION

Synthesis. 4-(3-((3-Methylamido)disulfanyl)propanoic acid) [2,2]paracyclophane was synthesized via a five-step procedure from commercially available [2,2]paracyclophane (Sigma-Aldrich, St. Louis, MO, USA). A schematic illustration of the synthetic route is shown in Scheme 1. Titanium(IV) chloride (8.4 mL, 77 mmol) (Sigma-Aldrich)

Scheme 1. Synthetic Route toward 4-(3-((3-Methylamido)disulfanyl)propanoic acid) [2,2]Paracyclophane

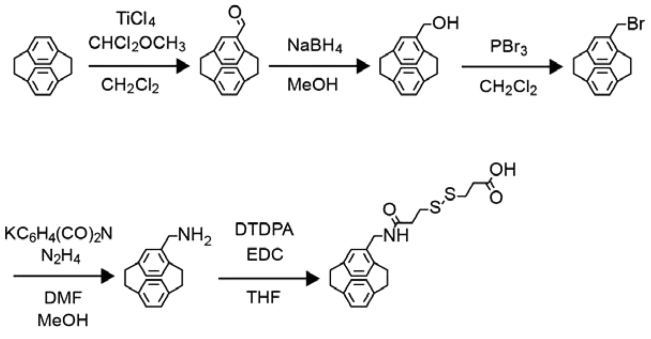

was added slowly to an ice-cooled solution of [2,2]paracyclophane (8.0 g, 38 mmol) in anhydrous CH_2Cl_2 (400 mL) under a nitrogen environment. The mixture was stirred for 20 min, followed by the dropwise addition of α,α-dichloromethyl methyl ether (4.0 mL, 44 mmol;Sigma-Aldrich). The reaction mixture was stirred at room temperature for 6 h, subsequently poured into water, and then stirred for an additional 2 h (200 mL). Next, the organic layer was washed with 3 M HCl (2 × 300 mL) and then with water (2 × 300 mL), after which it was dried over $MgSO_4$. After filtration and removal of the solvent, the crude product was purified on silica gel using hexane/CH_2Cl_2 (5/1) as the eluent to yield 4-formyl[2,2]paracyclophane as white crystals (6.6 g, 83%). The crystals were then dissolved in a mixture of MeOH (200 mL) and anhydrous tetrahydrofuran (THF; 10 mL). $NaBH_4$ (2.1 g, 28 mmol; Sigma-Aldrich) was added carefully to this solution, and the mixture was stirred at room temperature for 3 h. The excess $NaBH_4$ was then decomposed by the careful addition of water. The solution was then diluted with EtOAc (200 mL), washed with 3 M HCl (3 × 200 mL) and then with water (2 × 200 mL), and dried over $MgSO_4$. After filtration and removal of the solvent, 4-hydroxymethyl[2,2]paracyclophane was obtained as white crystals (6.0 g, 75%), which were used without further purification. The 4-hydroxymethyl[2,2]paracyclophane was dissolved in anhydrous CH_2Cl_2 (200 mL) and cooled to 0 °C under a nitrogen environment. Next, PBr_3 (3.00 mL, 31.8 mmol; Sigma-Aldrich) was added dropwise, and the mixture was stirred for 4 h. The reaction was hydrolyzed by the addition of water (150 mL), and the phases were separated. The organic layer was washed with 1 M HCl (150 mL), saturated $NaHCO_3$ solution (150 mL), and saturated NaCl solution (150 mL). It was then dried over $MgSO_4$ and filtered, after which the solvent was removed *in vacuo*. The crude product 4-bromomethyl[2,2]paracyclophane (5.81 g, 77%) was used in the next step without further purification. Crude 4-bromomethyl[2,2]paracyclophane and potassium phthalimide (3.71 g, 20.0 mmol; Sigma-Aldrich) were dissolved in dimethylformamide (100 mL) and heated to 80 °C for 4 h. After complete conversion (TLC control), the solvent was removed *in vacuo* and the residue was dissolved in EtOAc (500 mL) and washed with saturated NaCl solution (400 mL). The aqueous phase was extracted with CH_2Cl_2 (2 × 200 mL), and the combined organic phases were dried over $MgSO_4$. After removal of the solvent, the crude product (7.06 g) was dissolved in MeOH (300 mL) and hydrazine (19 mL, 80% in water; Sigma-Aldrich) was added. The reaction mixture was heated to 60 °C for 1 h (TLC control). Next, the solvent was removed, and the residue was taken up in CH_2Cl_2 (500 mL) and 1 M NaOH solution (300 mL). The phases were separated, and the aqueous phase was extracted with CH_2Cl_2 (300 mL). The combined organic phases were washed with 1 M NaOH (300 mL) and brine (300 mL). The organic phase was dried over $MgSO_4$, and the solvent was removed *in vacuo*. The crude product was purified on silica gel using CH_2Cl_2/MeOH (9/1) to yield 4-aminomethyl[2,2]paracyclophane (2.57 g, 56%). Next, 3,3′-dithiodipropionic acid (2.10 g, 10 mmol; Sigma-Aldrich) and *N*-ethyl-*N*′-(3-(dimethylamino)propyl)carbodiimide (EDC; 1.55 g, 10 mmol; Alfa Aesar, Ward Hill, MA, USA) were dissolved in anhydrous THF (250 mL) and stirred at room temperature for 20 min. 4-Aminomethyl [2,2]paracyclophane (2.37 g) was added to the resulting solution and reacted at room temperature for 12 h. The reaction product was washed with saturated $NaHCO_3$ solution (3 × 500 mL) and dried over $MgSO_4$. The crude product was purified on silica gel using hexane/ethyl acetate (5/1) to yield 4-(3-((3-methylamido)-disulfanyl)propanoic acid) [2,2]paracyclophane as white crystals (2.71 g, 63%). The following parameters were obtained from NMR, FT-IR, and ESI-MS analyses of the product. ^{1}H NMR (500 MHz, CDCl3, TMS): δ 6.67−6.69 (2d, J = 1.9 Hz, 1.9 Hz, 1H), 6.36−6.50 (m, 5H), 6.21 (d, J = 1.40 Hz, 1H), 5.71 (s, 1H), 4.35−4.40 (2d, J = 5.3 Hz, 5.3 Hz, 1H), 4.09−4.13 (2d, J = 5.2 Hz, 5.2 Hz, 1H), 2.72−3.47 (m, 16H), 2.52−2.55 (t, J = 14.1 Hz, 2H). ^{13}C NMR (125 MHz, CDCl3, TMS): δ 32.9, 33.0, 33.6, 33.8, 34.3, 34.9, 35.2, 35.7, 42.8, 129.1, 132.1, 132.2, 133.1, 133.2, 133.8, 135.1, 136.4, 138.0, 139.2, 139.3, 140.5, 170.8, 175.8. FT-IR (ATR; cm^{-1}): 3291 (m), 3024 (w), 2924 (m), 2853 (w), 1704 (s), 1668 (s), 1621 (m), 1520 (w), 1513 (m), 1444 (m), 1419 (m), 1332 (w), 1231 (w), 1204 (w), 1181 (w), 1041 (m), 940 (vw), 890 (vw), 823 (m), 762 (vw), 725 (vw), 624 (vw), 548 (w), 519 (m), 492 (w). ESI-MS: m/z (%) 428.15 (100) [M$^+$].

CVD Polymerization. The Parylene S−S coating was synthesized using a CVD polymerization process starting from the dimeric 4-(3-((3-methylamido)disulfanyl)propanoic acid) [2,2]paracyclophane. The dimer was first sublimated in the sublimation zone at approximately 125 °C. The sublimated species was then transferred in a stream of argon carrier gas at a flow rate of 30 cm^3(STP) min^{-1} to the pyrolysis zone, in which the temperature was controlled at 550 °C. Following pyrolysis, the radicals were transferred into the deposition chamber and then polymerized onto substrate materials on a rotating holder at 25 °C to ensure a uniform deposition of the Parylene S−S coating. The chamber wall was held at 90 °C to prevent any residual deposition. A pressure of 75 mTorr was maintained throughout the CVD polymerization process, and all deposition rates were regulated at approximately 0.5 Å/s, monitored on the basis of *in situ* quartz crystal microbalancing analysis (STM-100/MF, Sycon Instruments, East Styracuse, NY, USA).

Surface Characterizations. Author: Surface characterizations using a combination of infrared reflection absorption spectroscopy (IRRAS) and X-ray photoelectron spectroscopy (XPS) have confirmed the characteristic band vibrations and chemical compositions of the coating. IRRAS spectra were recorded using a 100 FT-IR spectrometer (PerkinElmer, Waltham, MA, USA) equipped with an advanced grazing angle specular reflectance accessory (AGA, PIKE Technolo-

DOI: 10.1021/acsami.5b03286
ACS Appl. Mater. Interfaces 2015, 7, 14431−14438

gies, Fitchburg, WI, USA) and a liquid nitrogen-cooled MCT detector. The samples were mounted in a nitrogen-purged chamber, and the recorded spectra were corrected for any residual baseline drift.The XPS measurements were carried out on a theta probe X-ray photoelectron spectrometer (Thermo Scientific, Hertfordshire, U.K.) with monochromatized Al Kα radiation as the X-ray source. The X-ray power was 150 kW, and the pass energies were 200.0 and 20.0 eV for the survey scan and the high-resolution (C 1s and S 2p) elemental scan, respectively. The atomic analysis of the XPS spectra was based on the atomic concentrations and was compared to theoretical values calculated on the basis of the structure.

Thiol-Redox and Disulfide Interchange Reaction. The switching and displacing ability of the Parylene S−S coated surfaces was achieved by altering the surface chemical compositions via disulfide interchange reactions with thiol-terminated molecules. Successful performance was then verified through conjugations with corresponding fluorescence tags. The surface function was first activated with carboxyl groups by the as-deposited coating of Parylene S−S, and a microcontact printing (μCP) process was used to bring the reactive sites between the substrate and a poly(dimethylsiloxane) (PDMS) stamp in conformal contact to confine the reaction locations. Before conducting the printing, the PDMS stamps were treated with 50 W of oxygen plasma for 2 min to render the surface hydrophilic. For the immobilization of fluorescein (FITC)-conjugated Arg-Arg-Arg-Gly-Asp (RRRGD) peptide (FITC-RRRGD) (Yao-Hong Biotechnology Inc., New Taipei City, Taiwan), a stamp with circular arrays of 50 μm diameter and a center−center spacing of 120 μm was inked with a solution containing 10 mM FITC-RRRGD and 5 mM EDC in distilled water and then printed on Parylene S−S coating for 6 h. The resulting samples were then washed with phosphate-buffered saline containing Tween 20 (PBS-Tween 20) (pH = 7.4; Sigma-Aldrich) three times, once more with pure PBS (pH = 7.4; Sigma-Aldrich), and finally rinsed with distilled water. Subsequently, 100 mM glutathione (GSH; Sigma-Aldrich) aqueous solution was incubated for 6 h in 25 °C with the samples to cleave the disulfide bond. PBS-Tween 20 and pure PBS were used to clean the resulting samples. The reduced samples were then imparted with amine functionality by incubating the samples in 100 mM 6-amine-1-hexanethiol (Dojindo, Kumamoto, Japan) aqueous solution in the presence of 1 mM 2,2′-dithiodipyridine (DTP; Sigma-Aldrich) for 6 h to complete the disulfide interchange cycle. A byproduct of pyridine-2-thione was formed during the reaction and was observed using a UV−vis spectrophotometer (Agilent Technologies, Santa Clara, CA, USA). The resulting samples were cleaned thoroughly three times with PBS-Tween 20 and one time with pure PBS. Successful addition of the amine groups was confirmed by fluorescence detection using Alexa Fluor 350 NHS ester (Life Technologies, Grand Island, NY, USA) aided by μCP during the conjugation process. The same disulfide interchange reaction was carried out on the same samples to install thiol-polyethylene glycol (PEG)-biotin (MW 5000; Nanocs, New York, NY, USA), and an Alexa Fluor 633 streptavidin was used for the detection. Finally, the chemical composition of the surfaces was restored to carboxyl functionality using the same interchange reaction cycle to install 3-mercaptopropionic acid (Sigma-Aldrich). Control experiments were performed in parallel on poly(4-*N*-hydroxy-succinimide ester-*p*-xylylene-*co*-*p*-xylylene) (NHS ester coating), poly(4-aminomethyl-*p*-xylylene-*co*-*p*-xylylene) (amine coating), and poly(4-*N*-maleimido-methyl-*p*-xylylene-*co*-*p*-xylylene) (maleimide coating) coated surfaces, for which FITC-RRRGD, Alexa Fluor 350 NHS ester, and Alexa Fluor 633 streptavidin were, respectively, used for the detection of the surface functionalities followed by the same redox conditions being compared to the disulfide interchange reaction to verify the covalent bonds are not subject to any cleavage. A fluorescence microscope (TE2000-U, Nikon) was used to examine the detection process. Each experiment was conducted in triplicate.

Wettability. Switched surface wettability experiments were performed on Parylene S−S coated silicon wafers using the aforementioned disulfide interchange reaction cycle to immobilize a hydrophobic molecule, 1H,1H,2H,2H-perfluorodecanethiol (50 mM; Sigma-Aldrich), and a hydrophilic peptide, Cys-Lys-Asp-Lys-Asp-Asp (CKDKDD) peptide (50 mM, Yao-Hong Biotechnology). A thorough wash process using deionized water was employed to clean the surface during each cleavage/immobilization step. The static water contact angle measurement on the resulting surfaces was performed at room temperature using a contact angle goniometer (First Ten Angstroms, Portsmouth, VA, USA) by placing 5 μL of distilled water on the surfaces. Each measurement was conducted in three different locations on the same sample and repeated for different samples in triplicate.

Cell Adhesion. Tissue culture polystyrene (TCPS) microplates (BD Falcon, Becton, Dickinson and Co., Franklin Lakes, NJ, USA) were coated with Parylene S−S, and the cell-repellent states were first prepared on the Parylene S−S coated TCPS by reacting them with an aqueous solution containing 400 mg/mL *O*-(2-aminoethyl)poly-(ethylene glycol) (amino-PEG; MW 5000; Sigma-Aldrich), with the addition of 5 mM EDC during the reaction. The cell-repellent surface modification during the disulfide interchange reaction was performed by reacting the plates with thiol-terminated PEG (400 mg/mL, MW 5000; Sigma-Aldrich). These reactions were maintained at 25 °C for 6 h. For the case of the cell-adherent surface modification, the Parylene S−S coated TCPS substrates were reacted with a 10 mM Arg-Gly-Asp-Tyr-Tyr-Cys (RGDYYC; Yao-Hong Biotechnology) aqueous solution at 25 °C for 6 h. The switchability between the cell-repellent surface and the cell-adherent surface was studied by first culturing cells onto the PEG-modified surfaces (Parylene S−S coated TCPS plates) with a seeding density of 6×10^4 cells/well. Two cell lines including commercially obtained 3T3 fibroblast cells (clone A31, CCL-163; ATCC, Manassas, VA, USA) and adipose-derived stem cells (ASCs) isolated from porcine adipose tissues (performed following institutional guidelines[30] and were provided by Prof. Shih-Torng Ding, Department of Animal Science and Technology, National Taiwan University, Taiwan) were used in the study. The cells were grown in Dulbecco's modified Eagle's medium (DMEM; HyClone, Logan, UT, USA) containing 10% fetal bovine serum (Biological Industries, Kibbutz Beit-Haemek, Israel) and 1% penicillin-streptomycin amphotericin B solution (catalog no. 03-033-1B; Biological Industries) at 37 °C in a humidified atmosphere containing 5% CO_2 and 95% air for 24 h. The switching between the cell-repellent and cell-adherent states was initiated using the aforementioned disulfide interchange reaction cycle to cleave/immobilize thiol-terminated PEG. The cells were then washed once with PBS (0.15 M, pH 7.4), detached by incubation with 0.5% trypsin/0.2% EDTA (Biological Industries), and resuspended with fresh culture medium. The resulting samples were then subjected to the disulfide interchange reaction to install RGDYCC, and subsequently new 3T3 cells, with the same seeding density (6×10^4 cells/well) and the same culture conditions, were cultured on the RGDYCC-modified plates. Four replicates per tested surface and three independent experiments were performed. A control experiment was performed in parallel using an NHS-ester coating to modify the TCPS plates with the same cell seeding density and culturing conditions. For cell counting, the cell suspensions were diluted in a 1:1 ratio with a 0.4% Trypan Blue solution (Sigma-Aldrich). The cell number and viability were determined by dye exclusion of live cells on a hemocytometer. The cell adhesion ratio was determined by dividing the number of cells on PEG- and/or RGD-immobilized surfaces with the number of cells on TCPS control surfaces. An inverted microscope (Olympus, Tokyo, Japan) was used to visualize the cell growth pattern for each step during the disulfide interchange cycle.

RESULTS AND DISCUSSION

The displaceable functional group of 3-((3-methylamido)-disulfanyl)propanoic acid was designed for the poly-*p*-xylylene coating (hereafter referred to as Parylene S−S coating) and was composed of an integrated disulfide moiety and a carboxylic acid end group. The functional group was first prepared as a substitution on the aromatic ring of the dimeric starting material [2,2]paracyclophane. The synthetic route is shown in Scheme 1, and the detailed characterizations of the starting

DOI: 10.1021/acsami.5b03286
ACS Appl. Mater. Interfaces 2015, 7, 14431−14438

materials are provided in the Experimental Section and the Supporting Information Figures S1−S3. Subsequently, the preparation of Parylene S−S coating was performed using a chemical vapor deposition (CVD) polymerization process with the dimeric starting material 4-(3-((3-methylamido)disulfanyl)-propanoic acid) [2,2]paracyclophane (Figure 1). During the

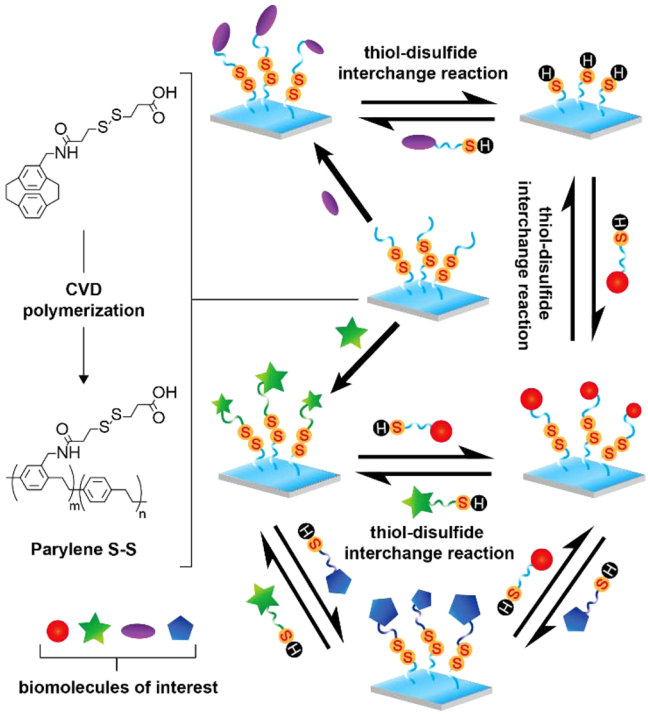

Figure 1. Schematic illustration of CVD polymerization to prepare Parylene S−S coating on material surfaces. The coating comprises an integrated disulfide moiety and a carboxylic acid end group, and it enables programmable switching between the immobilized biomolecules via the thiol−disulfide interchange reaction.

CVD polymerization, the starting material was sublimated at approximately 125 °C and then thermally treated at a pyrolysis temperature of approximately 550 °C. Pyrolytic cleavage occurred only for the two carbon−carbon bonds in the dimers and converted the dimers into quinonoid structures (monomers). The pyrolysis temperature was found to be critical for the quality of the resulting coatings. Finally, the monomers were spontaneously polymerized at room temperature (25 °C). The displaceable functional groups were compatible with the processing conditions during CVD polymerization; *i.e.*, decomposition or side reactions did not occur. A coating thickness of 50−150 nm was typically obtained, as estimated by *in situ* quartz crystal microbalancing (QCM). The as-deposited Parylene S−S coating was mechanically stable under a cross-cut tape adhesion test,[20] as well as a thermostability test carried out at 150 °C.[17]

Surface characterizations carried out using a combination of XPS and IRRAS confirmed the characteristic chemical compositions and structure of Parylene S−S coating. As indicated from the XPS survey spectra, Parylene S−S coating contained 88.53 at. % carbon, 5.74 at. % oxygen, 1.3 at. % nitrogen, and 4.43 at. % sulfur, which agree well with the theoretical values (79.31 at. % carbon, 10.35 at. % oxygen, 3.45 at. % nitrogen, and 6.89 at. % sulfur). The XPS high-resolution C 1 s spectra of Parylene S−S coating exhibited a signal at 285.0 eV, which can be attributed to the aliphatic and aromatic carbons (C−C, C−H). Additionally, the intensity of 80.7 at. % compared well with the theoretical concentration of 78.2 at. %. The characteristic signals at 285.3 eV (8.2 at. %), 286.0 eV (4.6 at. %), 288.8 eV (2.6 at. %), and 290.4 eV (2.4 at. %) correspond to C−S, C−N, O═C−N, and O═C−O bonds, respectively. A comparably low value of O═C−O (2.4 at. %, compared to a theoretical value of 4.4 at, %) was found due to the decomposition of carboxyl end groups during the CVD polymerization, while a consistent C−S value (8.2 at. %, compared to a theoretical value of 8.7 at. %) was showing the disulfide moiety was preserved intact. The signal at 291.4 eV (1.3 at. %) can be attributed to the $\pi \rightarrow \pi^*$ shakeup signal characteristic of aromatic π electrons and has been previously reported for other functionalized poly-*p*-xylylenes.[31] In addition, XPS high-resolution peak analysis was also performed for S 2p3/2 at 163.65 eV, and the spectra also have the characteristics of a disulfide form, as concluded by comparison with the literature.[32] The IRRAS spectra unambiguously confirmed the structural details of Parylene S−S coating, and the results are shown in Supporting Information. Two significant peaks at 1668 and 1704 cm^{-1} are attributed to the C═O asymmetric stretching bands of the amide bond and carboxyl acid end group, respectively. A broad band spanning from 3132 to 3544 cm^{-1}, indicative of a secondary N−H stretching mode of an amide bond and an O−H stretch of a carboxyl acid end group was also observed. Finally, the peaks at 1041, 1513, and 1621 cm^{-1}, which can be assigned to the C−N and N−H stretches of an amide bond, were detected as well. The XPS and IRRAS spectra are included in the Supporting Information Figures S4 and S5.

The switching and/or displacing ability of Parylene S−S coating was first achieved by dynamically altering its surface chemical composition. The attached functional molecule is detached from the surface under reduction conditions, and a new surface function is subsequently assembled by the disulfide interchange reaction to attach the second functional molecule. In this way, the biological function of the surface is correspondingly altered from one function to another. In this study, biomolecules including 6-amine-1-hexanethiol and thiol-terminated biotin (thiol-PEG-biotin) were used as examples, and their exchange was performed on identical samples of Parylene S−S coated substrates. The immobilizations were also compared in parallel to existing functional poly-*p*-xylylenes with nondisplaceable functional groups including NHS ester, amine, and maleimide, for which cleavage of the immobilized molecule is not possible once the covalent conjugation is formed. The surface function was first activated with carboxyl groups by the as-deposited coating of Parylene S−S, and fluorescein (FITC)-conjugated Arg-Arg-Arg-Gly-Asp (RRRGD) peptide was used to verify the availability of the carboxyl groups by forming amide bonds between the primary amines and the activated carboxyl groups through EDC-mediated conjugation. The immobilization was performed with the aid of a μCP process that was used to bring the reactive sites between the substrate and the PDMS stamp in conformal contact to confine the reaction locations.[33,34] The μCP process additionally served as a visual guide. As indicated in Figure 2a, the high-contrast fluorescein signal (green 50 μm diameter circle arrays) was detected in areas where FITC−RRRGD was printed using μCP. Displacement of the immobilized FITC−RRRGD with a second functional molecule was subsequently performed by introducing 6-amine-1-hexanethiol via the thiol−disulfide

DOI: 10.1021/acsami.5b03286
ACS Appl. Mater. Interfaces 2015, 7, 14431−14438

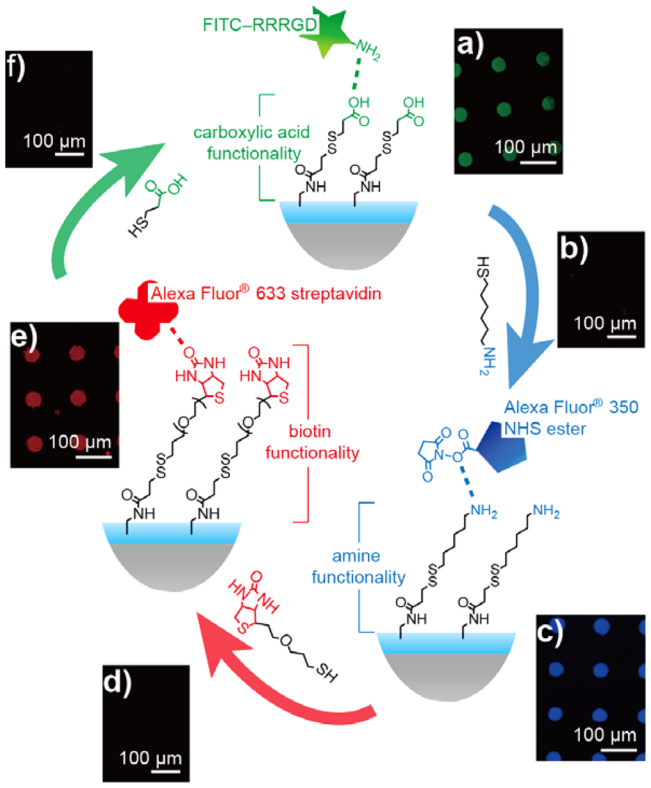

Figure 2. Fluorescent tags were used to verify the switching between altered surface chemical compositions. Fluorescently labeled molecules including FITC-RRRGD, Alexa Fluor 350 NHS ester, and Alexa Fluor 633 streptavidin were used to verify the surface functionalities of carboxylic acid, amine, and biotin, respectively, in a, c, and e. Cleavage of the disulfide upon installation of the new surface functionality was verified by the absence of fluorescence signals in b, d, and f. Surface modifications and the disulfide interchange reactions were performed on the same sample, which was coated with Parylene S–S.

interchange reaction, and the expected absence of the fluorescein signal was verified on the resulting displaced surface. Additionally, the attachment of 6-amine-1-hexanethiol was confirmed by reacting the surface with Alexa Fluor 350 NHS ester, which forms a rigid amide bond between the NHS ester moiety and the amine group. The results show high-contrast fluorescence signals (Alexa Fluor 350, blue circles), as displayed in Figure 2c. By contrast, for the nondisplaceable NHS ester-functionalized and amine-functionalized poly-*p*-xylylene coatings, firmly attached FITC–RRRGD and Alexa Fluor 350 NHS ester were respectively detected. They exhibited intense and comparable fluorescence signals before and after performing the same thiol–disulfide interchange reaction (see Supporting Information Figure S6a,b). The absence of nonspecific adsorption of the fluorescent molecules was confirmed by verifying that no Alexa Fluor 350 signal was detected on the amine-functionalized poly-*p*-xylylene coating as well as by performing the reaction on nonreactive poly-*p*-xylylene. The displacement activity was continued by repeated application of the thiol–disulfide interchange reaction and by introducing a thiol-PEG-biotin molecule to the sample surface. The successful attachment of the biotin molecules was verified by the detection of Alexa Fluor 633 streptavidin (high specific binding affinity toward biotin),[35] as shown in Figure 2e. Similarly, a control experiment was conducted in which thiol-PEG-biotin was reacted on a pure maleimide coating via the well-known thiol–maleimide coupling reaction.[36] The intensities of the Alexa Fluor 633 signals on such surfaces were found to be nearly constant even after the purposed treatment of the interchange reaction by high-concentration GSH (see the Supporting Information Figure S6c). The surface composition can always be reversibly switched to its original carboxyl functionality by displacement with 3-mercaptopropionic acid (Figure 2f). Verifications of the surface composition in each displacement step and the presence of thiols on the surface were conducted by using IRRAS analysis and UV–vis spectroscopy, respectively; the results were revealed in the Supporting Information Figures S7 and S8.

In a separate experiment, three subsequent switch cycles were examined for the immobilization of RRRGD by repeated applications of the disulfide redox and interchange processes. IRRAS spectra were recorded to assess the switching of the surface in response to each cycle (Figure 3a). Successful preparation of an RRRGD-rich state was verified by the presence of the characteristic amine (N–H) group peak at 3289 cm^{-1}. An RRRGD-free state was prepared in reduction conditions in a high concentration of GSH, which favored the production of oxidized glutathione (GSSG).[26,27] The presence of the RRRGD molecule on the surface was verified by

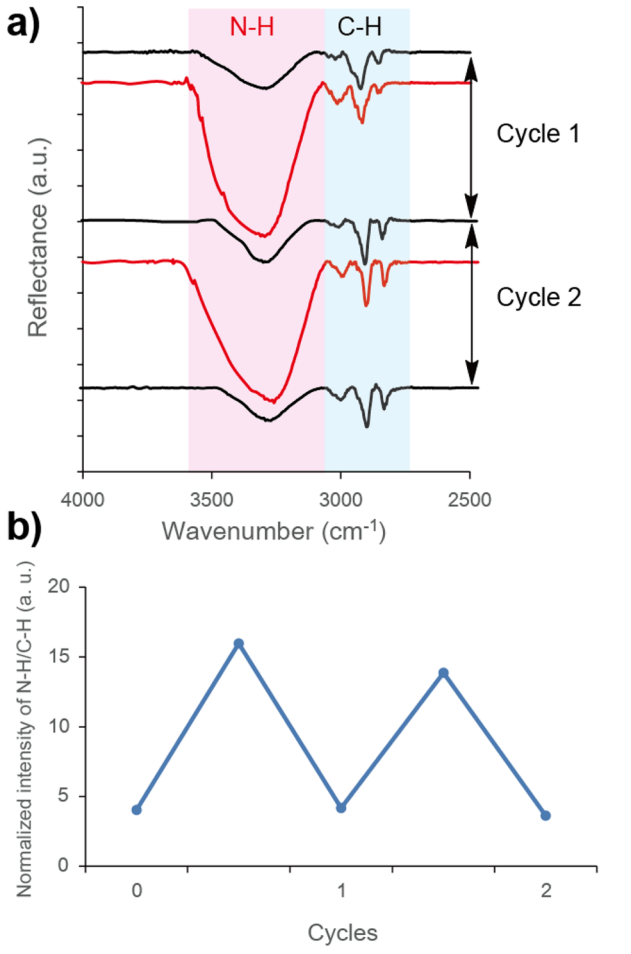

Figure 3. (a) IRRAS spectra recorded after each interchange reaction for the immobilized RRRGD. The peaks at approximately 3289 cm^{-1} are attributed to the characteristic bends of the RRRGD amine (N–H) group. (b) The normalized ratio of N–H/C–H indicates successful switching between an RRRGD-rich surface and an RRRGD-free surface.

DOI: 10.1021/acsami.5b03286
ACS Appl. Mater. Interfaces 2015, 7, 14431–14438

comparing the integrated peak intensities of the N−H and C−H bands. The ratio N−H/C−H used to estimate the relative amount of RRRGD was found to be in accordance with the switching phenomenon expected with each interchange cycle (Figure 3b), and a conversion rate of 87.0% from the RRRGD-rich state to the RRRGD-free state was estimated.

The observed rearrangements were further amplified into macroscopically detectable changes in the surface properties. Switching of the surface wettability was achieved through the interchange of a hydrophobic perfluorodecanethiol and a hydrophilic peptide, Cys-Lys-Asp-Lys-Asp-Asp (CKDKDD). Contact angles (CA) were measured for three subsequent switch cycles and revealed demonstrated reversibility between the hydrophobic (ca. 95 °CA) and hydrophilic (ca. 66 °CA) states (Figure 4). The hydrophobicity and hydrophilicity are

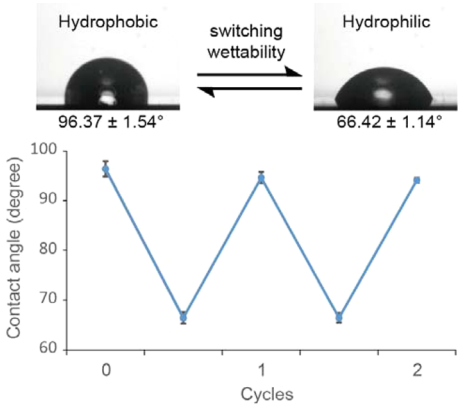

Figure 4. Switched surface wettability was confirmed by measuring the water contact angle over several switch cycles. The hydrophobicity and hydrophilicity of the surface is attributed to the attached perfluorodecanethiol and CKDKDD, respectively, for each cycle.

controlled by the surface chemical compositions of the assembled molecules of perfluorodecanethiol and CKDKDD, respectively. Scanning force microscopy did not reveal notable differences in surface roughness between systems configured with the two molecules, nor during the disulfide interchange processes, which reflects the behavior of a smooth surface for the studied systems. Future work may be conducted to generate a structured surface that can be integrated with the reported technology. Additionally, a superhydrophobic and superhydrophilic surface can be created based on the Wenzel model or the Cassie−Baxter model depending on the dimension of the surface structures.[37,38]

Finally, switchability of a more complex biointerface property, cell attachment on a material surface, was demonstrated. Programmed switching was carried out between a cell-adherent state and a cell-repellent state via the immobilization and interchange of two selected biomolecules: a thiol-terminated PEG (thiol-PEG) and a RGDYCC peptide. The growth of 3T3 fibroblast cells cultured for 24 h on the PEG-tethered Parylene S−S coated surface was found to be suppressed, which was expected due to the well-known property of the PEG motif as a repellent against cell adhesion.[39] The resulting surfaces were subsequently displaced by the interchange reaction to attach the thiol-rich RGDYCC peptide. The surface property was correspondingly converted to a cell-adherent state, as activated by RGD-mediated integrin interactions.[40] The two types of cell adhesion properties were alternated and confirmed for three subsequent switch cycles. Additionally, the cell viability of 3T3 cells in each cycle, as well as a confirmed switchability of cell adhesion for the cultured adipose-derived stem cells (ASCs), were demonstrated in the Supporting Information Table S1 and Figure S9, respectively. An intuitive control experiment was conducted in parallel by culturing 3T3 fibroblast on an amine-PEG-modified surface, where the modification was performed by immobilizing amine-PEG on a nondisplaceable coating of NHS ester-functionalized poly-*p*-xylylene. It was found that neither the interchange activity between different thiol molecules nor the switching between cell-adhesion states could be performed on such control surfaces (see the Supporting Information Figure S10). To further characterize the switchable cell adhesion, the number of cells on the surfaces was analyzed and shown to be consistent with obtained microscope images corresponding to each cycle of the cell growth pattern. A plot of the normalized cell numbers versus switch cycle, shown in Figure 5, unambiguously confirms the switching of dynamically manipulated cell adhesion.

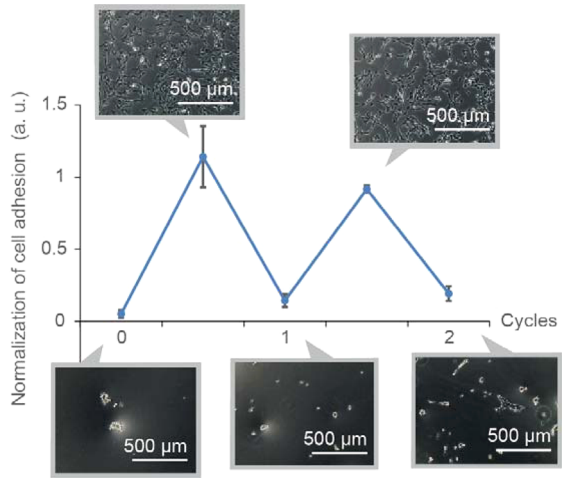

Figure 5. Examination of dynamically controlled cell adhesion on a material surface over several switch cycles. The surface modification was performed by switched immobilization between a thiol−PEG and a RGDYCC peptide using Parylene S−S coating. 3T3 fibroblast was used for the cell culture.

CONCLUSIONS

In summary, a new concept in poly-*p*-xylylene chemistry has been realized, mimicking the displaceable and dynamically controlled properties of real biological systems and able to fulfill the essential need for a tailored biointerface. The key features of this advanced version of poly-*p*-xylylene include the following: (i) There is a reversible mechanism for attaching/detaching biomolecules. For example, installed growth factor proteins[41] are cleaved when deactivation is required. Additionally, timed control of eluting drugs or biofunctional molecules from the material surfaces to enable the delivery of these molecules to the target sites is also possible. (ii) There is a mechanism of restoring biological functions with repeated cycles or a programmed displacement of new functions. Although the stability of the switching cycles may require further improvement through optimization of the redox conditions, the previously established library of functionalities and proven immobilization techniques are readily available for poly-*p*-xylylenes on the shelf.[31,42] Additionally, the fundamental

DOI: 10.1021/acsami.5b03286
ACS Appl. Mater. Interfaces 2015, 7, 14431−14438

aspects of the coating technology translate well from one substrate/application to another. Extensions of applications that employ the advanced poly-*p*-xylylene are only limited by the imagination.

■ ASSOCIATED CONTENT

Supporting Information

Figures showing ^{1}H NMR, ^{13}C NMR, and ESI-MS spectra of 4-(3-((3-methylamido)disulfanyl)propanoic acid) [2,2]-paracyclophane, XPS high-resolution C 1s and S 2p spectra of Parylene S−S coating, IRRAS characterizations of Parylene S−S coating, control experiments of nondisplaceable poly-*p*-xylylenes, UV−vis spectra of pyridine-2-thione side product, photographs of ASC cells growing on the surface and cell-adherent behavior, and photographs of control experiments for 3T3 fibroblast cells and a table listing cell adhesion and viability. The Supporting Information is available free of charge on the ACS Publications website at DOI: 10.1021/acsami.5b03286.

■ AUTHOR INFORMATION

Corresponding Author

*Fax: (+)886-2-33669476. E-mail: hsychen@ntu.edu.tw.

Author Contributions

†Z.-Y.G. and C.-Y.W. contributed equally to this work.

Notes

The authors declare no competing financial interest.

■ ACKNOWLEDGMENTS

H.-Y.C. gratefully acknowledges support from the Ministry of Science and Technology of Taiwan (Grants 101-2628-E-002-034-MY3 and 102-2911-I-002-507) and National Taiwan University (Grants 102R7745 and 103R7745).

■ REFERENCES

(1) Murphy, W. L.; McDevitt, T. C.; Engler, A. J. Materials as Stem Cell Regulators. *Nat. Mater.* **2014**, *13*, 547−557.

(2) Klee, D.; Höcker, H. Polymers for Biomedical Applications: Improvement of the Interface Compatibility. In *Biomedical Applications Polymer Blends*; Eastmond, G. C., Höcker, H., Klee, D., Eds.; Springer: Berlin, Heidelberg, 1999; Chapter 1, pp 1−57.

(3) Fisher, O. Z.; Khademhosseini, A.; Langer, R.; Peppas, N. A. Bioinspired Materials for Controlling Stem Cell Fate. *Acc. Chem. Res.* **2010**, *43*, 419−428.

(4) Stevens, M. M.; George, J. H. Exploring and Engineering the Cell Surface Interface. *Science* **2005**, *310*, 1135−1138.

(5) Sun, T.; Qing, G.; Su, B.; Jiang, L. Functional Biointerface Materials Inspired from Nature. *Chem. Soc. Rev.* **2011**, *40*, 2909−2921.

(6) Cole, M. A.; Voelcker, N. H.; Thissen, H.; Griesser, H. J. Stimuli-Responsive Interfaces and Systems for the Control of Protein−Surface and Cell−Surface Interactions. *Biomaterials* **2009**, *30*, 1827−1850.

(7) Yang, Y.-W.; Sun, Y.-L.; Song, N. Switchable Host−Guest Systems on Surfaces. *Acc. Chem. Res.* **2014**, *47*, 1950−1960.

(8) Stuart, M. A. C.; Huck, W. T. S.; Genzer, J.; Muller, M.; Ober, C.; Stamm, M.; Sukhorukov, G. B.; Szleifer, I.; Tsukruk, V. V.; Urban, M.; Winnik, F.; Zauscher, S.; Luzinov, I.; Minko, S. Emerging Applications of Stimuli-Responsive Polymer Materials. *Nat. Mater.* **2010**, *9*, 101−113.

(9) Dolbier, W. R., Jr.; Beach, W. F. Parylene-af4: A Polymer with Exceptional Dielectric and Thermal Properties. *J. Fluorine Chem.* **2003**, *122*, 97−104.

(10) Senkevich, J. J.; Mitchell, C. J.; Vijayaraghavan, A.; Barnat, E. V.; McDonald, J. F.; Lu, T.-M. Unique Structure/Properties of Chemical Vapor Deposited Parylene E. *J. Vac. Sci. Technol., A* **2002**, *20*, 1445−1449.

(11) Vaeth, K. M.; Jensen, K. F. Selective Growth of Poly(p-phenylene vinylene) Prepared by Chemical Vapor Deposition. *Adv. Mater.* **1999**, *11*, 814−820.

(12) Chen, H.-Y.; Lai, J. H.; Jiang, X.; Lahann, J. Substrate-Selective Chemical Vapor Deposition of Reactive Polymer Coatings. *Adv. Mater.* **2008**, *20*, 3474−3480.

(13) Zhang, C.; Thompson, M. E.; Markland, F. S.; Swenson, S. Chemical Surface Modification of Parylene C for Enhanced Protein Immobilization and Cell Proliferation. *Acta Biomater.* **2011**, *7*, 3746−3756.

(14) Jeon, B.-J.; Kim, M.-H.; Pyun, J.-C. Application of a Functionalized Parylene Film as a Linker Layer of SPR Biosensor. *Sens. Actuators, B* **2011**, *154*, 89−95.

(15) Ko, H.; Lee, E.-H.; Lee, G.-Y.; Kim, J.; Jeon, B.-J.; Kim, M.-H.; Pyun, J.-C. One Step Immobilization of Peptides and Proteins by Using Modified Parylene with Formyl Groups. *Biosens. Bioelectron.* **2011**, *30*, 56−60.

(16) Chen, H.-Y.; Rouillard, J.-M.; Gulari, E.; Lahann, J. Colloids with High-Definition Surface Structures. *Proc. Natl. Acad. Sci. U. S. A.* **2007**, *104*, 11173−11178.

(17) Nandivada, H.; Chen, H.-Y.; Bondarenko, L.; Lahann, J. Reactive Polymer Coatings that "Click. *Angew. Chem., Int. Ed.* **2006**, *45*, 3360−3363.

(18) Elkasabi, Y.; Chen, H.-Y.; Lahann, J. Multipotent Polymer Coatings Based on Chemical Vapor Deposition Copolymerization. *Adv. Mater.* **2006**, *18*, 1521−1526.

(19) Chen, H.-Y.; Lin, T.-J.; Tsai, M.-Y.; Su, C.-T.; Yuan, R.-H.; Hsieh, C.-C.; Yang, Y.-J.; Hsu, C.-C.; Hsiao, H.-M.; Hsu, Y.-C. Vapor-Based Tri-Functional Coatings. *Chem. Commun. (Cambridge, U. K.)* **2013**, *49*, 4531−4533.

(20) Sun, H.-Y.; Fang, C.-Y.; Lin, T.-J.; Chen, Y.-C.; Lin, C.-Y.; Ho, H.-Y.; Chen, M. H. C.; Yu, J.; Lee, D.-J.; Chang, C.-H.; Chen, H.-Y. Thiol-Reactive Parylenes as a Robust Coating for Biomedical Materials. *Adv. Mater. Interfaces* **2014**, *1*, No. 1400093.

(21) Wu, J.-T.; Huang, C.-H.; Liang, W.-C.; Wu, Y.-L.; Yu, J.; Chen, H.-Y. Reactive Polymer coatings: A General Route to Thiol-ene and Thiol-yne Click Reactions. *Macromol. Rapid Commun.* **2012**, *33*, 922−927.

(22) Chen, H.-Y.; Hirtz, M.; Deng, X.; Laue, T.; Fuchs, H.; Lahann, J. Substrate-Independent Dip-Pen Nanolithography Based on Reactive Coatings. *J. Am. Chem. Soc.* **2010**, *132*, 18023−18025.

(23) Chang, C.-H.; Yeh, S.-Y.; Lee, B.-H.; Hsu, C.-W.; Chen, Y.-C.; Chen, C.-J.; Lin, T.-J.; Hung-Chih Chen, M.; Huang, C.-T.; Chen, H.-Y. Compatibility Balanced Antibacterial Modification Based on Vapor-Deposited Parylene Coatings for Biomaterials. *J. Mater. Chem. B* **2014**, *2*, 8496−8503.

(24) Li, C.; Madsen, J.; Armes, S. P.; Lewis, A. L. A New Class of Biochemically Degradable, Stimulus-Responsive Triblock Copolymer Gelators. *Angew. Chem., Int. Ed.* **2006**, *45*, 3510−3513.

(25) Roy, D.; Cambre, J. N.; Sumerlin, B. S. Future Perspectives and Recent Advances in Stimuli-Responsive Materials. *Prog. Polym. Sci.* **2010**, *35*, 278−301.

(26) Szajewski, R. P.; Whitesides, G. M. Rate Constants and Equilibrium Constants for Thiol-Disulfide Interchange Reactions Involving Oxidized Glutathione. *J. Am. Chem. Soc.* **1980**, *102*, 2011−2026.

(27) Keire, D. A.; Strauss, E.; Guo, W.; Noszal, B.; Rabenstein, D. L. Kinetics and Equilibria of Thiol/Disulfide Interchange Reactions of Selected Biological Thiols and Related Molecules with Oxidized Glutathione. *J. Org. Chem.* **1992**, *57*, 123−127.

(28) Cuozzo, J. W.; Kaiser, C. A. Competition between Glutathione and Protein Thiols for Disulphide-Bond Formation. *Nat. Cell Biol.* **1999**, *1*, 130−135.

(29) Tian, F.; Lu, Y.; Manibusan, A.; Sellers, A.; Tran, H.; Sun, Y.; Phuong, T.; Barnett, R.; Hehli, B.; Song, F.; DeGuzman, M. J.; Ensari, S.; Pinkstaff, J. K.; Sullivan, L. M.; Biroc, S. L.; Cho, H.; Schultz, P. G.; DiJoseph, J.; Dougher, M.; Ma, D.; Dushin, R.; Leal, M.; Tchistiakova, L.; Feyfant, E.; Gerber, H.-P.; Sapra, P. A General Approach to Site-

DOI: 10.1021/acsami.5b03286
ACS Appl. Mater. Interfaces 2015, 7, 14431−14438

Specific Antibody Drug Conjugates. *Proc. Natl. Acad. Sci. U. S. A.* **2014**, *111*, 1766−1771.
(30) Williams, K.; Godke, R.; Bondioli, K. Isolation and Culture of Porcine Adipose Tissue-Derived Somatic Stem Cells. In *Adipose-Derived Stem Cells: Methods and Protocols*; Gimble, J. M., Bunnell, B. A., Eds.; Humana Press: New York, 2011; Chapter 7, pp 77−86.
(31) Lahann, J.; Langer, R. Novel Poly(*p*-xylylenes): Thin Films with Tailored Chemical and Optical Properties. *Macromolecules* **2002**, *35*, 4380−4386.
(32) Castner, D. G.; Hinds, K.; Grainger, D. W. X-ray Photoelectron Spectroscopy Sulfur 2p Study of Organic Thiol and Disulfide Binding Interactions with Gold Surfaces. *Langmuir* **1996**, *12*, 5083−5086.
(33) Xia, Y.; Whitesides, G. M. Soft Lithography. *Annu. Rev. Mater. Sci.* **1998**, *28*, 153−184.
(34) Perl, A.; Reinhoudt, D. N.; Huskens, J. Microcontact Printing: Limitations and Achievements. *Adv. Mater.* **2009**, *21*, 2257−2268.
(35) Caswell, K. K.; Wilson, J. N.; Bunz, U. H. F.; Murphy, C. J. Preferential End-to-End Assembly of Gold Nanorods by Biotin−Streptavidin Connectors. *J. Am. Chem. Soc.* **2003**, *125*, 13914−13915.
(36) Sletten, E. M.; Bertozzi, C. R. Bioorthogonal Chemistry: Fishing for Selectivity in a Sea of Functionality. *Angew. Chem., Int. Ed.* **2009**, *48*, 6974−6998.
(37) Forsberg, P.; Nikolajeff, F.; Karlsson, M. Cassie-Wenzel and Wenzel-Cassie Transitions on Immersed Superhydrophobic Surfaces under Hydrostatic Pressure. *Soft Matter* **2011**, *7*, 104−109.
(38) Sun, T.; Wang, G.; Feng, L.; Liu, B.; Ma, Y.; Jiang, L.; Zhu, D. Reversible Switching between Superhydrophilicity and Superhydrophobicity. *Angew. Chem., Int. Ed.* **2004**, *43*, 357−360.
(39) Zhang, M.; Desai, T.; Ferrari, M. Proteins and Cells on PEG Immobilized Silicon Surfaces. *Biomaterials* **1998**, *19*, 953−960.
(40) Hersel, U.; Dahmen, C.; Kessler, H. RGD Modified Polymers: Biomaterials for Stimulated Cell Adhesion and Beyond. *Biomaterials* **2003**, *24*, 4385−4415.
(41) Chen, Y.-C.; Sun, T.-P.; Su, C.-T.; Wu, J.-T.; Lin, C.-Y.; Yu, J.; Huang, C.-W.; Chen, C.-J.; Chen, H.-Y. Sustained Immobilization of Growth Factor Proteins Based on Functionalized Parylenes. *ACS Appl. Mater. Interfaces* **2014**, *6*, 21906−21910.
(42) Chen, H.-Y.; Lahann, J. Designable Biointerfaces Using Vapor-Based Reactive Polymers. *Langmuir* **2010**, *27*, 34−48.

DOI: 10.1021/acsami.5b03286
ACS Appl. Mater. Interfaces 2015, 7, 14431−14438